Appl. Phys. B (2012) 109:581–591
DOI 10.1007/s00340-012-5178-3

Applied Physics B
Lasers and Optics

Understanding the sensitivity of cavity-enhanced absorption spectroscopy: pathlength enhancement versus noise suppression

B. Ouyang · R. L. Jones

Received: 9 September 2011 / Revised: 11 July 2012 / Published online: 18 September 2012

Abstract Cavity-enhanced absorption spectroscopy is now widely used as an ultrasensitive technique in observing weak spectroscopic absorptions. Photons inside the cavity are reflected back and forth between the mirrors with reflectivities R close to one and thus (on average) exploit an absorption pathlength L that is $1/(1 - R)$ longer than a single pass measurement. As suggested by the Beer-Lambert law, this increase in L results in enhanced absorbance A (given by αL with α being the absorption coefficient) which in turn favours the detection of weak absorptions. At the same time, however, only $(1 - R)$ of the incident light can enter the cavity [assuming that mirror transmission T is equal to $(1 - R)$], so that the reduction in transmitted light intensity ΔI caused by molecular absorption equates to that would be obtained if in fact *no cavity were present*. The enhancement in $A = \Delta I/I$, where I is the total transmitted light intensity, achievable from CEAS therefore comes not from an increase in ΔI, but a sharp decrease in I. In this paper, we calculate the magnitudes of these two terms before and after a cavity is introduced, and aim at interpreting the sensitivity improvement offered by cavity-enhanced absorption spectroscopy from this observable-oriented (i.e. ΔI and I) perspective. It is first shown that photon energy stored in the cavity is at best as intense as the input light source, implying that any absorbing sample within the cavity is exposed to the same or even lower light intensity after the cavity is formed. As a consequence, the intensity of the light absorbed or scattered by the sample, which corresponds to the ΔI term aforementioned, is never greater than would be the case in a single pass measurement. It is then shown that while this "numerator" term is not improved, the "denominator" term, I, is reduced considerably; therefore, the increase in contrast ratio $\Delta I/I$ is solely contributed by the attenuation of transmitted background light I and is ultimately down to the suppression of any measurement noise that is associated with it. The noise component that is most effectively suppressed is the type whose magnitude scales linearly with light intensity I, as is typical of noise caused by environmental instabilities, followed by the shot noise which scales as square root of I. No suppression is achievable for noise sources that are independent of I, a notable example being the thermal noise of a detector or of detection electronics. The usefulness of this "noise suppression" argument is that it links the sensitivity gain offered by a cavity with the property of measurement noise present in the system, and clearly suggests that the achievable sensitivity is dependent on how efficient the various noise components are "suppressed" by the cavity.

B. Ouyang · R. L. Jones (✉)
Department of Chemistry, University of Cambridge,
Lensfield Road, Cambridge CB2 1EW, UK
e-mail: rlj1001@cam.ac.uk

1 Introduction

Cavity-enhanced techniques are widely used as an ultrasensitive tool in absorption spectroscopy. The first demonstration of cavity ring-down spectroscopy (CRDS) was made by O'Keefe and Deacon [1] using a pulsed laser light source. Following that, a large number of studies have been devoted to improving sensitivity and accuracy of the methodology and introducing variants which can be found, for example, in a recent review [2].

CRDS is not sensitive to pulse-to-pulse laser intensity fluctuation since it extracts information from the change of decay rate of the photon energy held in the cavity rather than the amount of light initially injected. For this reason

it has some significant advantages over the traditional absorption method in which any fluctuations of the laser intensity will be directly and usually linearly reflected in the retrieved absorption signal. As CRDS is a pulsed method by its nature, it fits well with the availability of pulsed lasers which are available in many spectral regions.

The use of lasers, however, brings challenges, most of them technical. For example, some CRDS measurements require efficient coupling of the laser frequency to one of the Fabry–Perot modes of the cavity, most commonly the TEM_{00}, and any slight drift of the laser frequency and/or cavity length will compromise this process. Additionally, many lasers are essentially monochromatic, or at best cover a relatively narrow wavelength range. Obtaining broad-band spectral coverage requires step scanning at the expense of time resolution.

Cavity-enhanced absorption spectroscopy (CEAS) is now widely used as an alternative pioneered by Engeln et al. [3] and O'Keefe [4]. In this method, a *cw* light source is used and the intensity of the light transmitted through the cavity is also measured in a continuous manner. The magnitude of intra-cavity extinction is derived from the attenuation of transmitted light intensity by the intra-cavity sample, using an approximate equation (see, e.g. Equation 9 in Ref. [5]). Since its advent, CEAS has found numerous applications in detecting trace species [5–15], studies of gas phase kinetics [16–21], capturing weak molecular transitions [22–26] and probing interfacial interactions [27–29] and molecular dynamics [30].

One of the major advantages of CEAS is that, when coupled to a suitable spectrometer, it can utilize a wide range of simple and compact *cw* light sources such as Xenon arc lamps, laser diodes and light emitting diodes. This is particularly attractive for field work as these are often much less demanding than lasers in terms of operation and servicing. The broad-band feature of these *cw* light sources and spectrometers means a wide spectral range can be covered without having to step-scan the wavelength of the light source. This then allows the retrieval of extinctions of multiple absorbing species using optimal fitting algorithms, e.g. of the kind which are widely used in differential optical absorption spectroscopy (DOAS) [31].

The most popular view of why a cavity enhances sensitivity is that, because of the high-reflectivity mirrors used in forming the resonant cavities, light will pass through the sample a large number of times, thus yielding a nominally long "absorption path length". For example, for cavities formed of two mirrors with reflectivity $R = 0.9999$, the "pathlength enhancement factor", which is widely accepted to be $1/(1 - R)$, has the value 10,000. This is taken to imply that a path length of 10 km can be achieved within a cavity length of 1 m.

While the above argument highlights the pathlength enhancement effect, it on the other hand neglects the fact that higher mirror reflectivity R necessarily comes with lower mirror transmission T, which means fewer photons will enter the cavity to exploit the pathlength enhancement. In qualitative terms this reduced signal implies a lower signal-to-noise ratio (if dominated by shot or thermal noise), and an important issue therefore is the extent of the tradeoff between higher R, implying longer absorption path length, and lower T, implying lower signal-to-noise ratio. This in many ways distinguishes CEAS from the more traditional long-path techniques such as the White or Herriott cells where light from the source is usually injected into the sample without such losses, and where every photon reaching the detector has traced the same path through the absorption cell.

Moreover, the CEAS community has long been aware of the issue that even if the reflectivity R of the cavity mirrors is held constant, enhancement factor of CEAS (when referenced to the single pass measurement) will have varying values which may change with, for instance, the intensity of the light incident on the detector and the detailed operational environment of the instrument. It is the purpose of this paper to further investigate this behaviour and provide some theoretical insight into the cause of this phenomenon.

This paper is organized as following. Firstly, in Sect. 2.1 we use a simple differential equation to describe how the photon intensity inside a cavity is built up following light injection with and without absorption/scattering of the sample. The key point, that intra-cavity photon intensity as well as the number of absorbed or scattered photons by the sample can never exceed those in a single pass measurement, can be readily derived.

Then, in Sect. 2.2, more rigorous expressions quantifying the various processes in the cavity are presented after removing the simplifying approximations made in the discussion in Sect. 2.1. Readers are nevertheless recommended not to be overly distracted by the detailed derivations in this section. Finally in Sect. 2.3, we derive explicit expressions to calculate the magnitude of both "signal" and "noise" in terms of the number of photons. This way it is clearly shown that the sensitivity of CEAS comes from the significantly reduced "noise" that is associated with the much weaker intensity of the light that now reaches the detector once a CEAS cavity is set up. We also demonstrate in this section that when there are different types of noise present in the measurement system, the sensitivity improvement provided by CEAS will vary and care should be taken when choosing the optimum mirrors to construct the cavity.

2 Results

2.1 A simple overview of signal and noise terms

We start with the simplest possible experimental arrangement in CEAS in which one has a cavity defined by two high reflectivity mirrors, a light source at one side of the cavity emitting photons and a detector at the other side capturing the photons transmitted through the cavity. Assuming initially an evacuated resonant cavity, once the injection light source is turned on, the instantaneous intra-cavity intensity will change as described by the following differential equation (e.g. [32]):

$$\frac{\mathrm{d}I^0_{\mathrm{cav}}}{\mathrm{d}t} = \frac{c}{d}\left[-I^0_{\mathrm{cav}}(1-R) + \gamma I_{\mathrm{in}}T\right]. \quad (1)$$

In Eq. (1), I^0_{cav} is the intensity within the empty cavity, I_{in} the intensity of the input light, c the speed of light, γ the mode coupling coefficient, d the mirror separation distance, and R and T are mirror reflectivity and transmittance. More explicitly, the first term on the right-hand side of Eq. (1) corresponds to the "loss" term, i.e. how many photons are lost per unit time from the cavity, and is therefore proportional to the product of the number of photons already trapped in the cavity (as it determines how many photons are incident on the cavity mirror per unit time) and $(1 - R)$ (as it determines the fraction of light that is lost, i.e. not reflected, every time it is incident on a mirror). The second term corresponds to the "source" term, i.e. how many photons are injected into the cavity per unit time, and should therefore be proportional to product of the intensity of the light source and the transmittance of the cavity mirror.

To simplify the analysis, we assume γ to be unity, which is its upper limit, in the following derivations. Deviation of γ from unity implicitly assumes that I_{in} is scaled by a constant and can be taken into account when required and does not affect the basis of the argument.

The solution to Eq. (1) is given by:

$$I^0_{\mathrm{cav}}(t) = \frac{I_{\mathrm{in}}T}{(1-R)}\left(1 - e^{-\frac{t}{\mathrm{d}/[c(1-R)]}}\right). \quad (2)$$

If it is further assumed that $T = (1 - R)$, Eq. (2) can be simplified to

$$I^0_{\mathrm{cav}}(t) = I_{\mathrm{in}}\left(1 - e^{-\frac{t}{\mathrm{d}/[c(1-R)]}}\right). \quad (3)$$

As an illustration, the build-up of cavity light intensities for cavities with two different mirror reflectivities is shown in Fig. 1 (with d set to be 1 m). As expected from Eq. (3), the intra-cavity light intensity tends in the limit to I_{in} in both cases, with the mirror reflectivity R merely defining the time to reach the steady-state value.

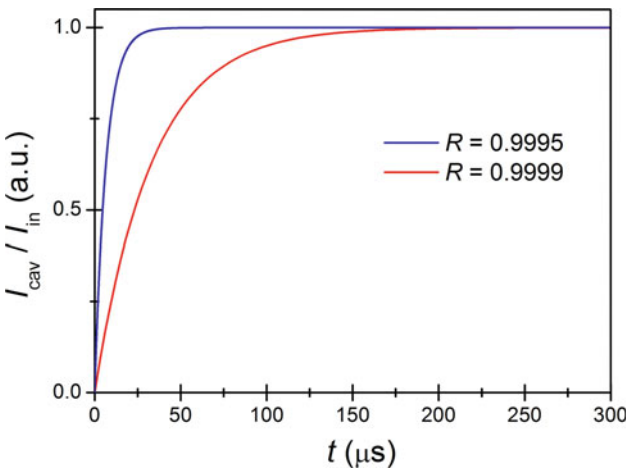

Fig. 1 Build-up curves of cavity intensity I_{cav} for mirror reflectivities $R = 0.9995$ and 0.9999 in the absence of any intra-cavity absorption/scattering. As is shown, the cavity intensity always reaches the input light intensity I_{in} irrespective of R

If we then introduce some absorbing or scattering species into the cavity, Eq. (1) becomes:

$$\frac{\mathrm{d}I_{\mathrm{cav}}}{\mathrm{d}t} = \frac{c}{d}[-I_{\mathrm{cav}}(1-R) - I_{\mathrm{cav}}\alpha d + I_{\mathrm{in}}T], \quad (4)$$

where α is the extinction coefficient of the sample. The second term in Eq. (4) accounts for the light loss due to sample extinction which is given by the product of I_{cav}, the intensity of the light that the sample is exposed to inside the cavity, and αd. Note that the superscript 0 has been dropped to distinguish I_{cav} in the presence of intra-cavity absorption/scattering from that for an empty cavity. The solution to Eq. (4) is:

$$I_{\mathrm{cav}}(t) = \frac{I_{\mathrm{in}}T}{(1-R+\alpha d)}\left(1 - e^{-\frac{t}{d/[c(1-R+\alpha d)]}}\right). \quad (5)$$

Again by assuming $T = (1 - R)$, Eq. (5) can be simplified to:

$$I_{\mathrm{cav}}(t) = \frac{I_{\mathrm{in}}}{[1+\alpha d/(1-R)]}\left(1 - e^{-\frac{t}{d/[c(1-R+\alpha d)]}}\right). \quad (6)$$

As shown in Eq. (6), the steady-state cavity intensity is now dependent on αd. Again for illustrative purposes, if we assume a weak absorption/scattering with $\alpha d = 1 \times 10^{-5}$, the build-up of cavity intensities for mirror reflectivities of $R = 0.9995$ and 0.9999 are as shown in Fig. 2.

A quick look at Fig. 2 suggests that the decrease in I_{cav} is larger in the higher R case, which may give the impression that the number of absorbed/scattered photons is increased using mirrors of higher R. However, this drop of steady-state I_{cav} is not equivalent to the number of photons removed by the absorbing/scattering sample (as will be explained below). Moreover, I_{cav} (and its change) is not what we directly observe as any photon detector has to

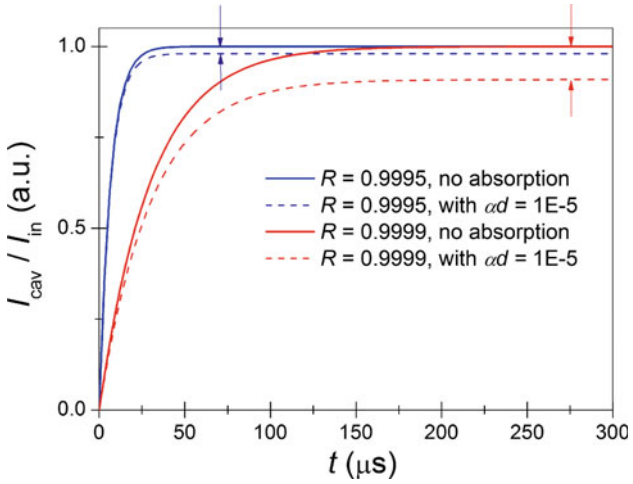

Fig. 2 Build-up curves of cavity intensities I_{cav} with intra-cavity absorption $\alpha d = 1 \times 10^{-5}$ for $R = 0.9995$ and 0.9999, respectively. For comparison, the curves for empty cavities are also plotted. It is evident (*arrows*) that the steady-state cavity intensity is more affected in the high R case than in the low one

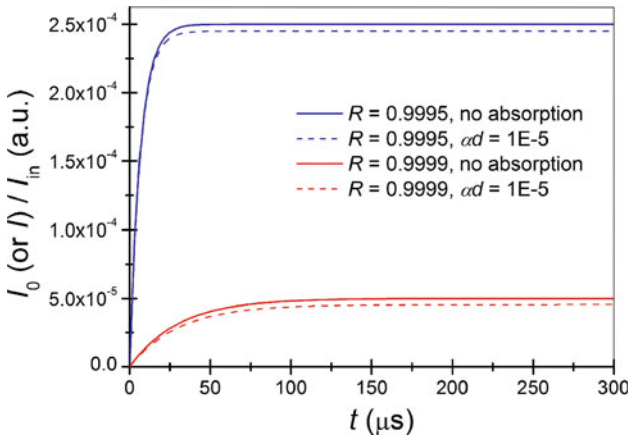

Fig. 3 The build-up curves of transmitted light intensities with intra-cavity absorption $\alpha d = 1 \times 10^{-5}$ for $R = 0.9995$ and 0.9999, respectively. For comparison, the curves for empty cavities are also plotted. It is clearly shown that the change in transmitted light intensity is approximately the same in both cavity cases

be placed outside the cavity and the observable quantity is the transmitted light I which is given by the product of $I_{cav} \times T$ or, $I_{cav} \times (1 - R)$ if $T = (1 - R)$ is assumed. This latter assumption can be violated under certain circumstances, for example when mirror absorption is not negligible for high R mirrors in the UV. The consequence of lifting this assumption will be discussed in more detail in the following section. It is also worth noting that light exiting the cavity can be probed only from one of the mirrors as the other has to be used to input light; for this reason, a scaling factor has to be applied to account for this effect. When mirror reflectivity is reasonably high (>0.9), the number of photons transmitted out of the cavity through each of the two mirrors is approximately the same and this scaling factor becomes ½. The time-dependent intensity transmitted through two cavities with mirror $R = 0.9995$ and 0.9999, respectively, are shown in Fig. 3. The decrease in the transmitted light intensity, ΔI, is given by

$$\Delta I = I_0 - I = (I^0_{cav} - I_{cav}) \times T/2, \tag{7}$$

where I_0 is the transmitted light intensity of an empty cavity and I is the transmitted light in the presence of intra-cavity extinction. Substituting the steady-state values of and I_{cav} from Eqs. (3) and (6), and assuming $T = (1 - R)$, Eq. (7) becomes:

$$\Delta I = \frac{\alpha d I_{in}}{2[1 + \alpha d/(1 - R)]}. \tag{8}$$

By applying Taylor expansion to the denominator and including only the first two terms, Eq. (8) becomes:

$$\Delta I = \frac{\alpha d I_{in}}{2}\left[1 - \frac{\alpha d}{(1 - R)}\right] \tag{9}$$

This result is $\alpha d/(1 - R)$ dependent. Therefore, the observed ΔI will vary with the ratio of αd to $(1 - R)$. However in cases when αd is small compared to $(1 - R)$, the second term in the square brackets in Eq. (9) becomes small compared to 1, serving as a relatively minor correction to the first term. This is illustrated in Fig. 3, where ΔI in the two cases are similar (to within 10 %, better shown below in Fig. 4), but the *absolute transmitted intensity* is significantly smaller in the higher R case.

The reason why the decreases in transmitted light remain approximately the same for different mirror reflectivities can be understood as following: as shown in Fig. 1, for an empty cavity, the steady-state light intensity I_{cav} is the same for all cavities independent of mirror reflectivity. If αd is small compared to $(1 - R)$, introduction of the absorbing sample incurs a measurable, yet relatively minor reduction of I_{cav}. For this reason, the steady-state I_{cav} is far less sensitive to the change of mirror reflectivity than I, and the intra-cavity sample is exposed to similar light intensities in the high and low R cases. The number of photons absorbed or scattered per unit time by the sample is thus very similar in these two cases.

Assuming the "source" term, i.e. the input light intensity remains unchanged before and after the sample is introduced, the cavity energy is lost via the transmission through both mirrors *plus* any extinction by the sample. In steady state, because energy is conserved, the decrease in the number of photons transmitted through both mirrors is necessarily equal to the number of photons absorbed or scattered by the sample, which as indicated above, is similar in the two R cases. One should, therefore, observe similar *change* (decrease) in transmitted light intensity in

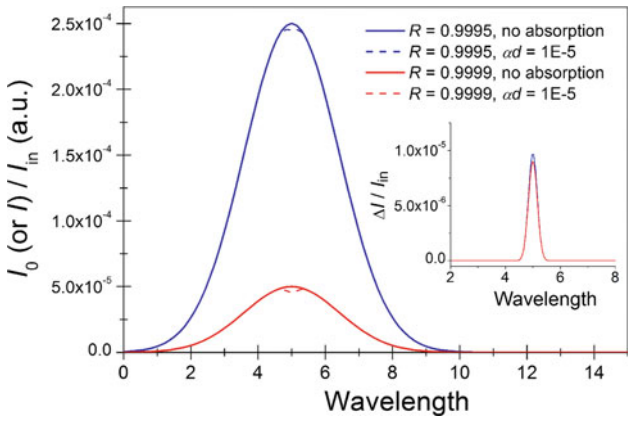

Fig. 4 Broad-band transmission spectrum from cavities with $R = 0.9995$ and 0.9999, respectively, in the absence (I_0, *solid lines*) and presence (I, *dotted lines*) of an assumed absorption feature with $\alpha d = 1 \times 10^{-5} e^{-(\lambda-5)^2/0.05}$, i.e. a Gaussian profile with λ being the wavelength. It is clear that despite a reduction by a factor of 5 in the absolute transmitted light intensity in the high reflectivity case, the number of photons absorbed by the sample (observed as the dips on the transmission spectrum) is similar in both cavities. This is more clearly shown in the inset graph where $\Delta I/I_{in}$ is plotted; the small difference between the two plots arises because the term $(1 - \alpha d/(1 - R))$ is slightly different in the two cases (0.9 vs. 0.98; cf. Eq. 9)

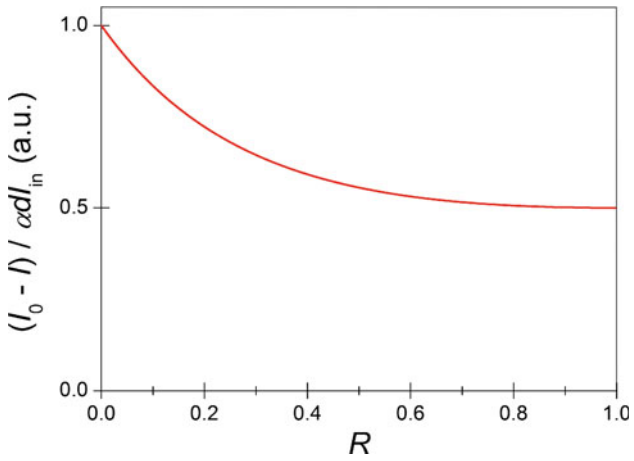

Fig. 5 The change of signal $(I_0 - I)$ (scaled by $\alpha d I_{in}$ with $\alpha d = 1 \times 10^{-7}$) with R varying from zero to near unity

both cases despite the fact that at higher mirror reflectivity, as shown in Fig. 3, the intensity of the total transmitted light is much lower, thus allowing the same "differential" structure to be recorded on a significantly attenuated background. This is evident in Fig. 4 where illustrative broad-band spectra are shown.

Finally, we note that the above discussions and results are restricted to high mirror reflectivity cases. Over a broader mirror reflectivity range, with a typical mirror reflectivity going all the way down to zero where we are effectively making a single pass measurement, the light intensity exiting each mirror is no longer equal, and the scaling factor will not be ½ as is assumed in Eq. (7). It is also interesting to consider the change of signal level, i.e. $(I_0 - I)$ and determine how it varies with R. A different equation has to be used to account for this "unsymmetrical" transmission of light through each mirror and is given in Eq. (25) in the following section. With αd set as 1×10^{-7} and $T = (1 - R)$, the resulting plot is shown in Fig. 5 which suggests that ΔI drops from $\alpha d I_{in}$, i.e. which one would achieve at the single pass case, and tends to approximately $\alpha d I_{in}/2$ after R exceeds ~ 0.5. This undesirable decrease (because of the fact that light exiting the cavity can only be probed from only one of the mirrors), as will be shown, is compensated by a simultaneous yet much quicker fall in noise due to the greatly attenuated absolute transmitted intensity, thus greatly improving the sensitivity in CEAS.

2.2 Quantitative assessment of cavity processes

While the principles outlined above are a valid description of CEAS characteristics, for a real experiment there are a number of additions required. For example, the relationship $T = (1 - R)$ does not necessarily hold, either due to mirror imperfections or because at extremely high mirror reflectivities [33] or in the deep UV region, mirror absorption (A) is no longer negligible, and T is instead given by $(1 - R - A)$. Moreover, it has been explicitly assumed, for example in Eqs. (1) and (4), that the light field intensity inside the cavity is homogenous. This presumption may be violated if the intra-cavity extinction becomes too large and/or if the mirror reflectivity is not close to unity. This section aims at quantifying the various cavity processes without making these approximations; however, readers are recommended not to be distracted from the main line of argument by the detailed derivations in this section.

We start by calculating the photon intensity inside the cavity. To this end we first consider photons travelling from the input (left) to the output (right) mirror. Along the cavity axis, the light intensity will decay by

$$\vec{I}(x) = \vec{I}(0)e^{-\alpha x} \tag{10}$$

due to sample extinction as dictated by Beer-Lambert law. In Eq. (10), the "$\rightarrow$" superscript indicates the direction of movement of the photons, α is the extinction coefficient of the intra-cavity species, x is the distance from the input mirror and $\vec{I}(0)$ is the intensity of right-moving light inside the cavity at the position of the input mirror whose coordinate x is set to 0.

We now consider the photons travelling in the opposite direction. The photons moving in this direction are those originally moving rightwards but which are reflected by the output mirror and hence change direction at the output

mirror. Moreover, as they move leftwards, their intensities will decay in the same way as the right-moving beam as shown in Eq. (10). This left-moving beam can therefore be written as

$$\overleftarrow{I}(x) = [\vec{I}(0)e^{-\alpha d} \times R] \times e^{\alpha(x-d)}, \tag{11}$$

where now the "$\leftarrow$" superscript indicates the leftwards moving direction of the photons.

The total light intensity at position x in the cavity, $I(x)$, can then be written as

$$I(x) = \vec{I}(x) + \overleftarrow{I}(x). \tag{12}$$

$I(x)$ will reach steady state when the injection and loss rates of photons reach equilibrium, i.e.

$$I_{\text{injection}} = I_{\text{loss}}. \tag{13}$$

The injection rate is simply given by

$$I_{\text{injection}} = I_{\text{in}} \times T. \tag{14}$$

The loss rate, as already noted in the preceding section, is the sum of two terms, one due to extinction by intra-cavity species and the other due to mirror losses (transmission plus absorption), i.e.

$$I_{\text{loss}} = I_{\text{abs/scatt}} + I_{\text{mirror}}. \tag{15}$$

The rate of absorption/scattering is determined by the intensity of photons that the molecules are exposed to and can be calculated as

$$I_{\text{abs/scatter}} = \int_0^d I(x)\alpha \mathrm{d}x = \vec{I}(0)(1 - e^{-\alpha d})(1 + \mathrm{Re}^{-\alpha d}) \tag{16}$$

by substituting Eqs. (10) and (11) into Eq. (12), multiplying by α and integrating with respect to the x coordinate according to Eq. (16). The rate of loss by mirror transmission and absorption is determined by the rate that photons are incident on the two mirrors and is given by

$$\begin{aligned} I_{\text{mirror}} &= (\overleftarrow{I}(0) + \vec{I}(d))(1 - R) \\ &= \vec{I}(0)e^{-\alpha d}(1 + \mathrm{Re}^{-\alpha d})(1 - R) \end{aligned} \tag{17}$$

by noting that the light loss from the input mirror is given by $\overleftarrow{I}(0)(1 - R)$ while that from the output mirror is given by $\vec{I}(d)(1 - R)$, with $\overleftarrow{I}(0)$ and $\vec{I}(d)$given by Eqs. (11) and (10) by setting $x = 0$ and d, respectively.

Substituting Eqs. (16) and (17) into (15) and then Eqs. (15) and (14) into (13), we have the following equation which links the intra-cavity intensity with that of the input light, i.e.

$$\vec{I}(0) = I_{\text{in}}T/(1 - R^2e^{-2\alpha d}). \tag{18}$$

The light probed by the detector, assuming (arbitrarily) a collection efficiency of one, is given by

$$I = T \times \vec{I}(d) = \frac{I_{\text{in}}T^2e^{-\alpha d}}{(1 - R^2e^{-2\alpha d})}, \tag{19}$$

where $\vec{I}(d)$ is obtained by substituting Eq. (18) into Eq. (10) with x set to d.

In the absence of intra-cavity extinction, i.e. when $\alpha = 0$, the light intensity is

$$I_0 = I_{\text{in}}T^2/(1 - R^2). \tag{20}$$

Dividing Eq. (20) by Eq. (19), we have

$$\frac{I_0}{I} = \frac{(1 - R^2e^{-2\alpha d})}{e^{-\alpha d}(1 - R^2)}. \tag{21}$$

After suitable re-arrangement, Eq. (21) gives an identical expression to calculate α as Eq. (4) derived by Fiedler et al. [34] despite the different approaches used.

Equation (21) is very general in that it applies even when intra-cavity absorption/scattering is so strong that a significant photon intensity gradient is formed along the cavity axis. It also holds if the cavity mirror reflectivity is not close to 1, which means a large fraction of light can exit the cavity after just one pass and consequently the light moving in opposite directions inside the cavity is considerably different. Both conditions are rare in typical CEAS practices and approximations can be made which shall give

$$\frac{(I_0 - I)}{I} = \alpha \times \frac{d}{(1 - R)}, \tag{22}$$

where the term $d/(1 - R)$ is often represented as "effective optical pathlength" by works in CEAS. After suitable arrangement of this equation, we end up with the widely used expression to calculate absorption coefficient in CEAS as

$$\alpha = \left(\frac{I_0 - I}{I}\right) \times \frac{(1 - R)}{d}. \tag{23}$$

We should also note that a collection efficiency of unity for light exiting the cavity has been explicitly assumed in the above derivations. This is obviously an optimistic approximation; however, a lower than unity collection efficiency would affect both CEAS and a single pass experiment, and will thus have comparable effects when comparing the S/N of the two methods. It is not therefore relevant to the tenor of the arguments here.

2.3 Calculations of the signal-to-noise ratio enhancement

2.3.1 Quantification of detected signal

When measuring a spectrum, the 'signal' in the context of this paper is taken to be the change in the number of

transmitted photons due to the introduction of the sample, i.e.

$$\text{signal} = (I_0 - I) \tag{24}$$

which for CEAS, ignoring optical and detection efficiency factors and using Eqs. (19) and (20) becomes

$$\text{signal} = \frac{I_{\text{in}} T^2 (1 - e^{-\alpha d})(1 + R^2 e^{-\alpha d})}{(1 - R^2)(1 - R^2 e^{-2\alpha d})}. \tag{25}$$

Equation (25) is perhaps too complex for ready interpretation. However, if one divides this equation by Eq. (16) and assumes $R \cong 1$ and $T = (1 - R)$, it emerges that

$$\frac{I_0 - I}{I_{\text{abs}}} \cong \frac{1}{2}. \tag{26}$$

This is in line with the necessity of conserving energy in the whole process, as has been argued in Sect. 2.1, i.e. any photons lost in absorption/scattering events will result in the same decrease in the number of transmitted photons through cavity mirrors. The scaling factor ½ is, as stated previously, due to the fact that only half of the exiting light can be probed in CEAS because the detector is positioned behind only one of the cavity mirrors.

Another important result is that at the limit of $R \to 1$ and $T = (1 - R)$, Eq. (25) reduces to

$$\text{signal} = \frac{I_{\text{in}}(1 - e^{-\alpha d})}{2}\left[1 - \frac{1 - e^{-\alpha d}}{(1 - R)}\right] \tag{27}$$

which again shows that the "signal" term in CEAS is that of a single pass measurement (outside the square brackets in the above equation) scaled by a factor (in the square brackets). At the limit of $\alpha d \ll (1 - R)$, this factor approaches 1 and the signal term in CEAS becomes a half of that of the single pass measurement as has been demonstrated above.

2.3.2 *Quantification of measurement noise*

Sources of noise in optical absorption measurements can be broadly categorized in three types:

The first type, referred to as environmental noise hereafter, is caused by unstable environmental conditions such as the change of the emission spectrum of the light source due to, e.g. drifts in source temperature. Other typical environmental noise sources include undesirable lensing effects when the flowing sample does not possess a uniform distribution of temperature or density, and misalignment of optical path due to pressure differentials, mechanical vibrations, etc. For a linear optical system, the magnitude of this type of noise is assumed to scale linearly with that of the absolute light intensity.

The second type is shot noise which originates as a statistical phenomenon as there is always a spread associated with the average number of probed photons. In consequence, there is always a spread in the number of generated photon carriers in the detector. Shot noise instead has been well-known to scale as the square root of the light intensity [35].

The third type is also associated with the detector, but in contrast to the shot noise, its magnitude does not change with light intensity. A typical example is the thermal noise of the photon detector and any associated electronics for the conversion of the photon generated signals.

The dependence of the magnitude of the above noise sources, denoted as δI, on the absolute light intensity can therefore be explicitly written as

1. Type 1 noise
$$(\delta I)_1 = a \times I \tag{28}$$

2. Type 2 noise
$$(\delta I)_2 = b \times I^{1/2} \tag{29}$$

3. Type 3 noise
$$(\delta I)_3 = c \tag{30}$$

with a, b and c being proportionality coefficients that vary among instruments and their operational environments.

2.3.3 *Quantification of the signal-to-noise ratio enhancement of CEAS*

Evaluation of signal and noise terms requires knowledge of both I_0 and I; therefore, the noise of both needs to be considered. For simplicity, here we assume that the noise of I_0 can be sufficiently reduced compared to I and can therefore be neglected by suitable averaging (i.e. we can take a suitably large number of repeated measurements for I_0 and then average them). Inclusion of the contribution of noise from I_0 will result in a more complex derivation, but as its neglect does not affect the arguments in the paper, it is not given here.

It can then be seen from Eq. (22) that the signal-to-noise ratio can be written as

$$\text{S/N} = \frac{\alpha}{\delta\alpha} = \frac{(I_0 - I)}{\left(\frac{I_0}{I} \times \delta I\right)}. \tag{31}$$

In the case of weak intra-cavity extinction, $I_0 \cong I$ and Eq. (31) can be obtained simply by dividing Eq. (24) by δI. This is in agreement with the intuitive picture, i.e. $(I_0 - I)$ is the change caused by the intra-cavity sample which gives the "signal" while δI is the sum of all three types of noises

as outlined in Eqs. (28)–(30). The CEAS enhancement factor, Q, is given by the ratio of S/N of CEAS and that of a single pass measurement, i.e.

$$Q = \frac{(S/N)_{\text{CEAS}}}{(S/N)_{\text{single}}}. \tag{32}$$

Care should be taken when calculating S/N and Q using Eqs. (31) and (32), given that it can have different dependence on I as shown in Eqs. (28)–(30). To examine this, we adopt three scenarios, each with one type of noise dominating. After substituting Eqs. (21), (25) and (28) or (29) or (30) into Eq. (31), it is possible to calculate Q under each scenario. Note that the noise for a single pass measurement $(\text{S/N})_{\text{single}}$ can be calculated simply by assuming $R = 0$.

In the first scenario where δI scales linearly with I, we have the Q of CEAS being

$$Q_1 = \frac{(1 + R^2 e^{-\alpha d})}{(1 - R^2 e^{-2\alpha d})}. \tag{33}$$

In the second scenario, we assume the dominant noise to be the shot noise and the Q of CEAS is now given by

$$Q_2 = T \frac{(1 + R^2 e^{-\alpha d})}{(1 - R^2 e^{-2\alpha d})\sqrt{(1 - R^2 e^{-2\alpha d})}}. \tag{34}$$

For the third scenario, the dominant noise has no dependence on I as shown in Eq. (30), and Q of CEAS is given by

$$Q_3 = T^2 \frac{(1 + R^2 e^{-\alpha d})}{(1 - R^2 e^{-2\alpha d})^2}. \tag{35}$$

These results take more familiar forms at the limit of $\alpha d \to 0$ and $R \to 1$ as shown below:

$$(Q_1)_{\substack{\alpha d \to 0 \\ R \to 1}} = \frac{1}{(1 - R)} \tag{36}$$

$$(Q_2)_{\substack{\alpha d \to 0 \\ R \to 1}} = \frac{T}{(1 - R)} \times \frac{1}{\sqrt{2(1 - R)}} \tag{37}$$

$$(Q_3)_{\substack{\alpha d \to 0 \\ R \to 1}} = \frac{T^2}{(1 - R)^2} \times \frac{1}{2}. \tag{38}$$

To further simplify the above results, we again assume $T = (1 - R)$, and Eqs. (36)–(38) can now be simplified to $1/(1 - R)$, $1/\sqrt{2(1 - R)}$ and 1/2, respectively. This second result has been derived previously by Fiedler et al. [33, 36, 37], where shot noise was assumed as the only noise type present in the measurement. It is apparent from Eqs. (33) to (38) that CEAS will have enhancement factors which vary widely for different noise sources. For example for $R = 0.9999$, we obtain enhancement factors of 10,000, 71 and 0.5, respectively, for the three noise cases. It is evident that CEAS does not provide *any* enhancement when detector thermal noise dominates, as CEAS is unable to reduce this noise by reducing the light intensity I.

In reality, all three noise sources are generally present and the enhancement factor of CEAS therefore typically lies somewhere between these three limits. Taking a mirror reflectivity ranging from 0 (a single pass) to 1, as R is increased, the cavity throughput decreases continuously while once R reaches $\sim$0.5 the *change* of the cavity throughput caused by cavity absorption/scattering remains approximately constant (see Fig. 5). The type 1 noise (often) exceeds type 2 shot noise at the earlier stage, i.e. when R is not particularly large and hence the intensity of light transmitted through the cavity is strong, given that the ratio of the two types of noise scales as the square root of the light intensity (cf. Eqs. 28, 29). However, type 1 noise, as it scales linearly rather than with the square root of intensity, falls more rapidly than shot noise as the cavity throughput is decreased by increasing mirror reflectivity. Therefore, a transition point will eventually be reached if a high enough R is used. This is shown qualitatively in Fig. 6. The pertinent point is that there is a cross-over point in the contributions of these two noise sources. The location of this point depends on the specific nature of the noise sources and in this simulated case, it occurs at $R = 0.9995$.

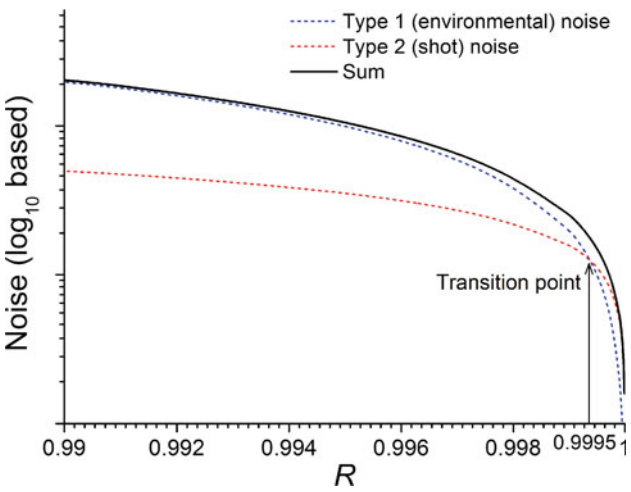

Fig. 6 Shift of the overall noise from being controlled by the type 1 (environmental) noise to being controlled by the shot noise when R is increased. The cross-over point is dependent on the detailed parameterization of coefficients a and b (as in Eqs. 28, 29) and will thus vary significantly between different experimental setups. In this simulated case, it occurs at $R = 0.9995$ which is what we found for one of our cavities operating around 660 nm in the red visible region [38]. The type 3 (detector thermal) noise is not included in this figure, mainly because if it is the dominant noise, increasing mirror R will offer no sensitivity improvement and is thus of less interest

2.3.4 Measurement accuracy and precision

Another major difference between type 1 and type 2 noises is that they generally occur on different time scales. This can be appreciated by examining the properties of coefficients a and b in Eqs. (28) and (29).

The coefficient b of shot noise is a constant once the detector bandwidth is defined [35]; therefore, it introduces random noise at all time points in a measurement series. However, type 1 noise, which results from environmental instabilities, is more complex as it can be composed of both random and quasi-periodic noise depending on how the environment changes. A typical example of the periodic noise is temperature drift of the light source, causing its emission spectrum to fluctuate in a quasi-periodic manner. If this occurs at a slower periodicity than the signal sampling, it will generate a fluctuating baseline and will mainly affect measurement accuracy. On the other hand, high frequency type 1 noise will merge with shot noise and mainly affect the precision of the measurements.

The use of a cavity thus improves both measurement accuracy and measurement precision by suppressing both types 1 and 2 noises. If a mirror reflectivity is selected which is at a higher reflectivity than the transition point in Fig. 6, the quasi-periodic fluctuation of the measurement baseline (type 1 noise) would become less noticeable but measurement precision may still be improved by further suppressing the shot noise. It is also apparent that, by continuing to increase mirror reflectivity and hence reducing cavity throughput, there will finally be a stage when the detector thermal noise exceeds the shot noise. If this is the case, using even higher mirror reflectivity will offer no further gain in S/N (as the thermal noise is independent of intensity change, cf. Eq. 30). This is obviously a region where CEAS should avoid working and is thus not included in Fig. 6.

3 Discussion and conclusion

It sounds counter-intuitive to argue that the signal strength, when defined as the number of photons actually absorbed or scattered by a sample, has in fact decreased after introducing a cavity. However, this is an inevitable consequence of the current light input method, i.e. the light has to pass through the highly reflective mirror before it is coupled into the cavity, thus resulting in a very low injection efficiency. Therefore, the advantage of improving sensitivity using high reflective mirrors is offset by the low transmission of these mirrors. However, as is shown above, the presence of the cavity greatly suppresses the total transmitted light, potentially leading to a substantially improved measurement S/N. Therefore, the enhancement, or under the theme of this paper, "suppression" ability of a cavity will depend not only on its mirror reflectivity but also on the specific types of noise (and their relative magnitudes) that are present in the measurement.

It is also noteworthy that most of the discussions in this paper have been restricted to cases where αd, i.e. intra-cavity extinction per pass, is small compared to $(1 - R)$, because most applications are primarily interested in the ability of detecting very weak absorption. As αd gradually gets larger and exceeds $(1 - R)$, both the signal (Eq. 25) and the noise terms (Eqs. 28–30) will be affected. However, with some knowledge of the strength of intra-cavity absorption, it is still possible to calculate the optimum R using Eqs. (33)–(35). An often neglected fact is that the optimum mirror reflectivity depends on the type of the dominant noise in the measurement and should be treated with care, ideally with some quantification of the different type of noise contributions for a cavity under its specific operational environment.

In fact, the choice of mirror reflectivity is always of intense interests to experimentalists; for this reason it may be helpful to further discuss the determination of optimum mirror reflectivity for practical CEAS measurements. We start with the dominant noise being of type 1. This is often the case when mirror reflectivity is low as shown in Fig. 6 and/or when the input intensity I_{in} is high when strong light sources such as coherent laser are being used [as the ratio of type 1 (linear) to type 2 (shot) noise scales as $I^{1/2}$]. Under these circumstances, as indicated by Eq. (36), increasing R will generally improve sensitivity, and CEAS will then yield an improvement of minimum detectable absorption by a factor of $1/(1 - R)$ which is often inaccessible to White and Herriott cells. It is also noteworthy that in the type 1 noise dominated domain, mirror transmission T has no effect on the enhancement factor Q at the limit of $\alpha d \to 0$, and one should always aim at using highest possible reflectivity mirrors to improve sensitivity. A potential complication with increasing R is the change of cavity finesse/mode structure which will in turn affect the coupling coefficient γ in Eq. (1). This is difficult to calculate using theoretical models, but for incoherent light sources such as light emitting diodes, our empirical tests show that γ stays within the range 0.5–1.0 and does not vary significantly with varying R. Coherent light sources such as lasers may be more demanding with regard to mode coupling and should thus be considered with extra care. However, it appears that γ ranges between 0.1 and 1.0 depending on the detailed optical setups and it is not unreasonable to expect γ to reach the high end of the range when suitable injection method such as off-axis [32] is adopted.

When sufficiently large mirror reflectivities are used, the effects of type 1 noise will eventually fall below those of

type 2 (shot) noise, as shown in Fig. 6. This appears to have been observed by, e.g. Thalman and Volkamer [13], although the authors did not mention noise origin in their measurements. On the other hand, mid-infrared measurements by Moyer et al. [39], as well as our studies at visible wavelengths have both shown some residual type 1 noise caused by, for example, the fluctuation of laser baseline power, semi-stable etalons and cavity misalignment caused by pressure differential on an instrument used on an aircraft platform (in Moyer et al.) and by temperature instability of the light source resulting in quasi-periodic drift of the emission spectrum (in our case). All these observations show the interplay between the two different types of noises in typical CEAS measurements, and it is expected that the enhancement factor Q will fall between the two limiting values given by Eqs. (36) and (37) at the limit of $\alpha d \rightarrow 0$. It is also worth noting that the sensitivity of CEAS is *linearly* proportional to the transmission T of the mirror (cf. Eq. 37) in the type 2 shot noise dominated region; therefore, cavities formed of mirrors with comparable reflectivities may have sharply different sensitivities, which highlights the importance of transmission T in evaluating high reflectivity mirrors.

In terms of practical optical configurations, our group along with many others has used incoherent light sources coupled with an off-confocal placement of cavity mirrors (in order to achieve near-continuum transmission of the broadband input light [40]). An alternative to this is the off axis-integrated cavity output spectroscopy (OA-ICOS) where the light, often from a *cw* laser, is injected in an off-axis manner to the cavity mirror in order to relax the stringent stability requirement for cavity distance or laser frequency [32]. Other differences between the two CEAS arrangements include but are not limited to the collimation quality of the beam, the varying intensities of the light sources as well as the different optical components used. All these are expected to have impacts on the injection and collection efficiencies of the light beam which will in turn affect the relative weighting of the three types of noise in the measurements. Despite these apparent differences, however, photon intensity held in the cavity remains no greater than that of the input light, and following this argument it is expected that the core arguments proposed above stay valid for both CEAS variants.

We end the paper by concluding that from a signal-to-noise analysis perspective, CEAS gains its sensitivity by allowing the weak absorption structure to be recorded on a significantly reduced, and thus much less noisy background. Optimum instrument performance is thus achieved by considering cavity mirror reflectivity in conjunction with sample optical depth and practical aspects such as relative contributions of different noise types which may be present.

Acknowledgments We wish to thank the Natural Environmental Research Council for postdoctoral research fellowship to BO under the RONOCO consortium (University of Cambridge Grant Award RG50086). We also wish to express thanks to the two anonymous reviewers for their helpful and constructive comments on the manuscript.

References

1. A. O'Keefe, D.A.G. Deacon, Rev. Sci. Instrum. **59**, 2544–2551 (1988)
2. G. Berden, R. Engeln (eds.), *Cavity Ring-Down Spectroscopy: Techniques and Applications* (Wiley, New York, 2009)
3. R. Engeln, G. Berden, R. Peeters, G. Meijer, Rev. Sci. Instrum. **69**, 3763–3769 (1998)
4. A. O'Keefe, Chem. Phys. Lett. **293**, 331–336 (1998)
5. T. Gherman, D.S. Venables, S. Vaughan, J. Orphal, A.A. Ruth, Environ. Sci. Technol. **42**, 890–895 (2008)
6. J.M. Langridge, S.M. Ball, R.L. Jones, Analyst **131**, 916–922 (2006)
7. J.M. Langridge, T. Laurila, R.S. Watt, R.L. Jones, C.F. Kaminski, J. Hult, Opt. Express **16**, 10178–10188 (2008)
8. S.M. Ball, J.M. Langridge, R.L. Jones, Chem. Phys. Lett. **398**, 68–74 (2004)
9. I. Courtillot, J. Morville, V. Motto-Ros, D. Romanini, Appl. Phys. B Lasers Opt. **85**, 407–412 (2006)
10. V.L. Kasyutich, C.S.E. Bale, C.E. Canosa-Mas, C. Pfrang, S. Vaughan, R.P. Wayne, Appl. Phys. B Lasers Opt. **76**, 691–697 (2003)
11. M. Triki, P. Cermak, G. Mejean, D. Romanini, Appl. Phys. B Lasers Opt. **91**, 195–201 (2008)
12. T. Wu, W. Zhao, W. Chen, W. Zhang, X. Gao, Appl. Phys. B Lasers Opt. **94**, 85–94 (2009)
13. R. Thalman, R. Volkamer, Atmos. Meas. Tech. **3**, 1797–1814 (2010)
14. W. Denzer, M.L. Hamilton, G. Hancock, M. Islam, C.E. Langley, R. Peverall, G.A.D. Ritchie, Analyst **134**, 2220–2223 (2009)
15. S. Vaughan, T. Gherman, A.A. Ruth, J. Orphal, Phys. Chem. Chem. Phys. **10**, 4471–4477 (2008)
16. V.L. Kasyutich, C.E. Canosa-Mas, C. Pfrang, S. Vaughan, R.P. Wayne, Appl. Phys. B Lasers Opt. **75**, 755–761 (2002)
17. C. Pfrang, M.T.B. Romero, B. Cabanas, C.E. Canosa-Mas, F. Villanueva, R.P. Wayne, Atmos. Environ. **41**, 1652–1662 (2007)
18. S. Vaughan, C.E. Canosa-Mas, C. Pfrang, D.E. Shallcross, L. Watson, R.P. Wayne, Phys. Chem. Chem. Phys. **8**, 3749–3760 (2006)
19. W.X. Zhao, X.M. Gao, L.Q. Hao, M.Q. Huang, T. Huang, T. Wu, W.J. Zhang, W.D. Chen, Vib. Spectrosc. **44**, 388–393 (2007)
20. K. Maeda, S.R.T. Neil, K.B. Henbest, S. Weber, E. Schleicher, P.J. Hore, S.R. Mackenzie, C.R. Timmel, J. Am. Chem. Soc. **133**, 17807–17815 (2011)
21. S. Crunaire, J. Tarmoul, C. Fittschen, A. Tomas, B. Lemoine, P. Coddeville, Appl. Phys. B Lasers Opt. **85**, 467–476 (2006)
22. J. Ye, L.S. Ma, J.L. Hall, J. Opt. Soc. Am. B Opt. Phys. **15**, 6–15 (1998)
23. M.J. Thorpe, J. Ye, Appl. Phys. B Lasers Opt. **91**, 397–414 (2008)
24. B. Bakowski, L. Corner, G. Hancock, R. Kotchie, R. Peverall, G.A.D. Ritchie, Appl. Phys. B Lasers Opt. **75**, 745–750 (2002)

25. H.R. Barry, L. Corner, G. Hancock, R. Peverall, T.L. Ranson, G.A.D. Ritchie, Phys. Chem. Chem. Phys. **5**, 3106–3112 (2003)
26. D.J. Hamilton, M.G.D. Nix, S.G. Baran, G. Hancock, A.J. Orr-Ewing, Appl. Phys. B Lasers Opt. **100**, 233–242 (2010)
27. L. van der Sneppen, G. Hancock, C. Kaminski, T. Laurila, S.R. Mackenzie, S.R.T. Neil, R. Peverall, G.A.D. Ritchie, M. Schnippering, P.R. Unwin, Analyst **135**, 133–139 (2009)
28. M. Schnippering, S.R.T. Neil, S.R. Mackenzie, P.R. Unwin, Chem. Soc. Rev. **40**, 207–220 (2010)
29. A.A. Ruth, K.T. Lynch, Phys. Chem. Chem. Phys. **10**, 7098–7108 (2008)
30. S.R.T. Neil, K. Maeda, K.B. Henbest, M. Goez, R. Hemmens, C.R. Timmel, S.R. Mackenzie, Mol. Phys. **108**, 993–1003 (2010)
31. U. Platt, J. Stutz, *Differential Optical Absorption Spectroscopy: Principles and Applications*, 1 edn. (Springer, Berlin, 2008)
32. J.B. Paul, L. Lapson, J.G. Anderson, Appl. Optics **40**, 4904–4910 (2001)
33. S.E. Fiedler, A. Hese, U. Heitmann, Rev. Sci. Instrum. **78**, 073104 (2007)
34. S.E. Fiedler, A. Hese, A.A. Ruth, Chem. Phys. Lett. **371**, 284–294 (2003)
35. G.C. Bjorklund, M.D. Levenson, W. Lenth, C. Ortiz, Appl. Phys. B Photophys. Laser Chem. **32**, 145–152 (1983)
36. S.E. Fiedler, A. Hese, A.A. Ruth, Rev. Sci. Instrum. **76**, 023107 (2005)
37. S.E. Fiedler, A. Hese, A.A. Ruth, Rev. Sci. Instrum. **76**, 089901(E) (2005)
38. O.J. Kennedy, B. Ouyang, J.M. Langridge, M.J.S. Daniels, S. Bauguitte, R. Freshwater, M.W. McLeod, C. Ironmonger, J. Sendal, O. Norris, R. Nightingale, S.M. Ball, R.L. Jones, Atmos. Meas. Tech. **4**, 1759–1776 (2011)
39. E.J. Moyer, D.S. Sayres, G.S. Engel, J.M.S. Clair, F.N. Keutsch, N.T. Allen, J.H. Kroll, J.G. Anderson, Appl. Phys. B Lasers Opt. **92**, 467–474 (2008)
40. R. Engeln, G. vonHelden, G. Berden, G. Meijer, Chem. Phys. Lett. **262**, 105–109 (1996)